

CHEMICAL INVESTIGATIONS OF IMPACT FEATURES ON SAMPLE 12001, 520 AND MICROCRATER SIMULATION EXPERIMENTS. K. Nagel, H. Fechtig, A. El Goresy, Max-Planck-Institut für Kernphysik, Heidelberg/W. Germany and N. Grögler, Physikalisches Institut, Bern / Switzerland.

Investigations on sample 12001,520 were focused mainly on the chemistry of glass and metal spherules. They include: 1) Semiquantitative measurements using a scanning electron microscope (SEM) with a Si(Li) solid state detector, and 2) quantitative electron microprobe analyses. The solid state detector measured compositional variations of metallic spherules adhering to the glass surface and of a glass splash surrounding the largest crater on the surface. A separate piece of the sample was used for quantitative measurements of the glass matrix and of metallic inclusions in the substrate. The results of the quantitative microprobe analyses, given in Table 1, show strong variations in sulphur concentrations within individual spheres (based on standard deviations). This observation was confirmed by SEM analyses of 7 spherules adhering to the glass surface. These spherules, one of which is shown in Fig. 1, were particularly sulphur enriched near the surface. To explain the chemical variations, an assumption was made that the spherules contain several phases, as implied by the metallic FeNi core and a troilite boundary. Similar spherules have been found in the glass linings of a polished crater section of sample 65315,68. These observations are in agreement with the dependence of the Ni/Fe ratios of metallic particles of this sample as a function of particle diameter (similar to ratios in FeNi residues in some lunar microcraters (1)). The variability of the Ni/Fe ratios and sulphur content of metal spherules with spherule sizes may, however, be a function of the electron beam's penetration depth, i.e. the location of the excited area in the metal particle. In small metal spherules the excited area may include the whole particle whereas in large ones the electron beam may not have penetrated to the Ni rich metal core. Thus, it is to be expected that large particles show lower Ni/Fe ratios and higher sulphur contents than small particles. In order to check this interpretation, measurements were performed on several spherules at various excitation potentials. By reducing the excitation voltage from 30 keV to 10 keV the Ni/Fe ratio was found to decrease continuously while the sulphur content was increasing. The crumbled edges may be directly due to the enrichment of troilite at the boundary of the spherules (Fig. 1). Simulation experiments using a dust accelerator, iron projectiles and glass target showed that in the projectile velocity range between 2 and 3 km/s the projectile is partially welded to the glass and exhibits a lip or "halo". In multiphase spherules, this halo, consisting of the brittle troilite, may be crumbled, as in Fig. 1. However, we have no explanation for the concentration of troilite at the particle boundaries. Fig. 2 shows the Co Ni composition fields for metal particles. (A, coarse anorthosites; B, Apollo 12 and 15 mare basalts; C, the meteoritic range (2)) incorporating our Ni and Co measurements of the metallic inclusions (Table 1). The correlation of Ni and Co of these analyses suggests a homogenization of previously heterogeneous metallic particles.

Twenty-six point analyses of the glass sample indicate an extremely homogenized melt. The average composition is (wt%): 46.3 SiO₂, 14.4 Al₂O₃, 14.3 FeO, 11.2 MgO, 10.3 CaO, 2.74 TiO₂, 0.47 Na₂O, 0.30 Cr₂O₃, 0.24 MnO. The homogeneity is

CHEMICAL INVESTIGATIONS OF IMPACT FEATURES.....

K. Nagel et al.

further indicated by a constant ratio of the K/Ca as observed during a degassing experiment of ^{39}Ar of another piece of this sample (3). Several glass splashes were found on the surface of sample 12001,520. A particularly interesting one with radial features surrounding several small particles (Fig. 3) ($\leq 20 \mu\text{m}$ in diameter) welded to the glass surface was chemically investigated using a Si(Li) detector in the SEM. Chemical analyses of the larger particle indicated the presence of Al, Si and Ca, with admixtures of particles enriched in Fe and Cr, and Fe and Ti, respectively. The smaller particles consisted of Fe and Cr, or Fe and Ti. The radial splash material surrounding the particles is composed primarily of Mg, Al, Ca, Ti and Fe. These elemental ratios correspond to a homogenized glass matrix. Accordingly the particles probably did not originate from the matrix, because of their unusual composition, but rather represent projectile residues. Based on the compositions of the glass splash and the particles in the center, this feature seems to be genetically related to the formation of a crater including target and projectile material. Various alternatives could be proposed to explain the splash feature and the neighbouring three craters: 1) the splash could have originated during the formation of the large crater; 2) the larger crater next to the splash is younger than the radial splash form. The large crater has perturbed the continuity of the radial structure although radial features continue beyond the outer edges of the large crater. Furthermore no Cr and Fe or Ti and Fe rich particles were detected in the large crater. Such particles were only encountered in the two smaller craters. Hence it seems plausible to conclude that the large crater was formed after development of the splash thus disturbing it on its south east side. It is worthwhile to mention that the fused crater glass in the smallest crater contains melted CrFe and TiFe rich particles, while in the middle crater such particles reside on the surface of the glass. For these reasons we believe that the splash originated during the formation of the smallest crater via a Ti, Cr, and Fe rich projectile. The unusual enrichment in Cr, Ti, and Fe may suggest a lunar projectile rather than a meteoritic.

Diameter (D) to depths (T) ratios of well developed circular craters of sample 12001,520 have been published (4). A histogram of these D/T measurements confirmed former results (5) in displaying 3 distinct peaks. Suitable simulation experiments relate the first peak of $D/T = 1.3$ to iron micrometeorites; the second peak of $D/T = 2.0$ to impacts by stony meteorites; and the third peak of $D/T = 2.6$ to impacts by low density projectiles. Iron projectiles on metal targets were used in the simulation experiments to obtain convincing results (6). Additional simulation experiments (7) using iron projectiles on feldspar targets at velocities of 5, 7.5 and 10 km/s confirm earlier results (6). Other experiments used Al and Fe projectiles (8) in the velocity range of 2 to 11 km/s and stated a disagreement with our results (6,7).

To clarify this discrepancy, more simulation experiments were performed using Fe projectiles on glass targets in the velocity range of 2.3 to 16.9 km/s. In Fig. 4 the T/D ratios are plotted as a function of the projectile velocity for glass and bytownite targets (7). After an increase of T/D below 4 km/s impact velocity, the new results indicate T/D to be independent of velocity above 4 km/s. We therefore feel that both results agree well.

CHEMICAL INVESTIGATIONS OF IMPACT FEATURES

K. Nagel et. al

REFERENCES:

- (1) K. Nagel et al. (1975), Proc. Lunar Sci. Conf. 6th, p. 3417-3432. (2) J.I. Goldstein (1975), Proc. Lunar Sci. Conf. 6th, p. 343-362. (3) S.A. Guggisberg (1977), Ph. D. Thesis, Bern. (4) H. Fechtig et al. (1977), Proc. Lunar Sci. Conf. 8th, p. 889-899. (5) K. Nagel et al. (1976), Proc. Lunar Sci. Conf. 7th, p. 1021-1029. (6) V. Rudolph (1968), Z. Naturforsch. 24a, p. 326-331. (7) K. Nagel et al. (1976), Earth Planet. Sci. Lett. 30, p. 234-240. (8) J.F. Vedder and J.C. Mandeville (1974), J. Geophys. Res. 79, p. 3247-3256.

Table 1: quantitative microprobe measurements.

Fe	Ni	Co	P	S	Total
89.93	7.38	0.72	0.90	0.35	99.27
0.68	0.07	0.11	0.06	0.29	
91.36	1.29	-	3.53	3.10	99.28
0.63	0.10	-	0.29	0.45	
89.28	1.17	0.26	7.17	0.66	98.54
1.36	0.09	0.06	0.39	0.30	

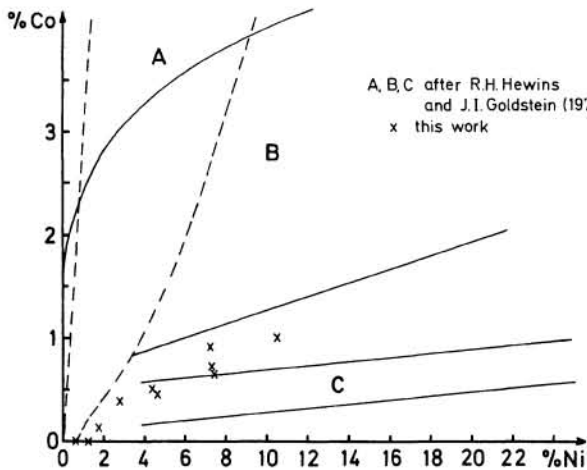


Fig. 2

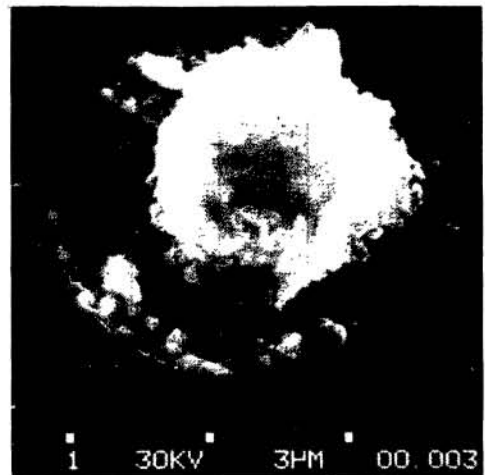


Fig. 1

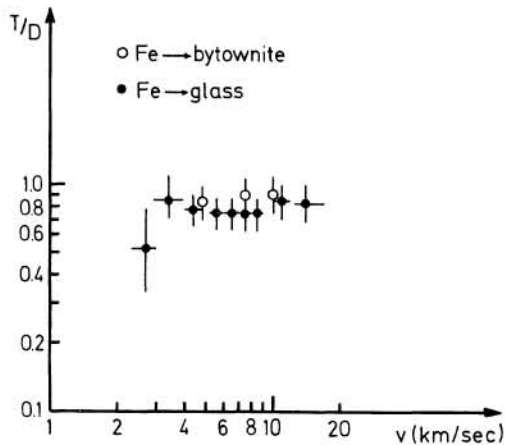


Fig. 4

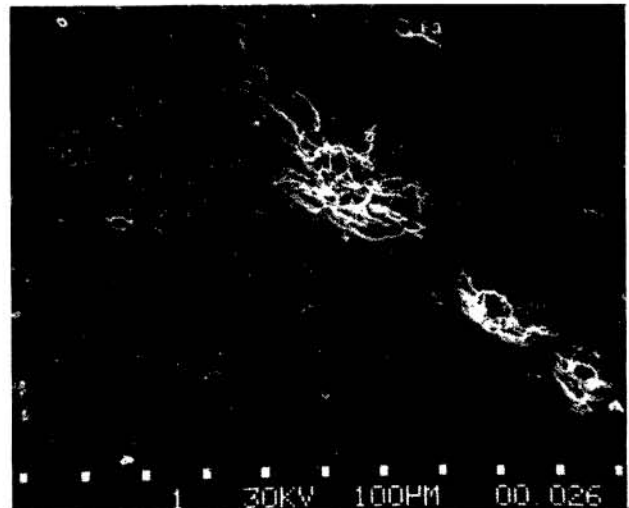


Fig. 3